The Plant Cell, Vol. 26: 729–740, February 2014, www.plantcell.org

The Synaptonemal Complex Protein ZYP1 Is Required for Imposition of Meiotic Crossovers in Barley[W][OPEN]

Abdellah Barakate,[a,1] James D. Higgins,[b,1,2] Sebastian Vivera,[a] Jennifer Stephens,[c] Ruth M. Perry,[b] Luke Ramsay,[c] Isabelle Colas,[c] Helena Oakey,[a] Robbie Waugh,[a,c] F. Chris H. Franklin,[b] Susan J. Armstrong,[b,3] and Claire Halpin[a,3,4]

[a] Division of Plant Sciences, College of Life Sciences, University of Dundee at The James Hutton Institute, Invergowrie, Dundee DD2 5DA, United Kingdom

[b] School of Biosciences, University of Birmingham, Edgbaston, Birmingham B15 2TT, United Kingdom

[c] The James Hutton Institute, Invergowrie, Dundee DD2 5DA, United Kingdom

ORCID IDs: 0000-0001-6027-8678 (J.D.H.); 0000-0001-6980-9906 (I.C.); 0000-0002-1808-8130 (C.H.)

In many cereal crops, meiotic crossovers predominantly occur toward the ends of chromosomes and 30 to 50% of genes rarely recombine. This limits the exploitation of genetic variation by plant breeding. Previous reports demonstrate that chiasma frequency can be manipulated in plants by depletion of the synaptonemal complex protein ZIPPER1 (ZYP1) but conflict as to the direction of change, with fewer chiasmata reported in *Arabidopsis thaliana* and more crossovers reported for rice (*Oryza sativa*). Here, we use RNA interference (RNAi) to reduce the amount of ZYP1 in barley (*Hordeum vulgare*) to only 2 to 17% of normal zygotene levels. In the *ZYP1*^{RNAi} lines, fewer than half of the chromosome pairs formed bivalents at metaphase and many univalents were observed, leading to chromosome nondisjunction and semisterility. The number of chiasmata per cell was reduced from 14 in control plants to three to four in the ZYP1-depleted lines, although the localization of residual chiasmata was not affected. DNA double-strand break formation appeared normal, but the recombination pathway was defective at later stages. A meiotic time course revealed a 12-h delay in prophase I progression to the first labeled tetrads. Barley ZYP1 appears to function similarly to ZIP1/ZYP1 in yeast and *Arabidopsis*, with an opposite effect on crossover number to ZEP1 in rice, another member of the Poaceae.

INTRODUCTION

Meiosis consists of two successive nuclear divisions, which result in the production of four haploid daughter cells (Zickler and Kleckner, 1998; Cnudde and Gerats, 2005). Meiotic division I is preceded by DNA replication, a process that generates a pair of sister chromatids from each original chromosome. Physical connections between homologous chromosome pairs (homologs) during prophase I ensure their accurate disjunction and reductional segregation to opposite cell poles, and recombination between the homologs generates genetic variation. The second, mitotic-like division, results in the equational segregation of the sister chromatids to form the four haploid gametes. Meiotic recombination is initiated by the formation of numerous programmed DNA double-strand breaks (DSBs) by the topoisomerase II–related protein SPO11 during early prophase I (Keeney et al., 1997; Grelon et al., 2001; Hartung et al., 2007). In most species, including plants, only a small proportion (~5%) of the DSBs result in the formation of genetic crossovers (COs) with the remainder repaired as noncrossovers (NCOs). Extensive studies in budding yeast (*Saccharomyces cerevisiae*) have shown that the majority of COs are dependent on a set of proteins referred to as ZMMs (the zipper proteins Zip1, Zip2, Zip3, Zip4; the MutS homologs Msh4 and Msh5; and Mer3 [meiotic recombination 3]) (reviewed in Lynn et al., 2007). ZMM-dependent COs exhibit interference, a phenomenon whereby a CO occurring at a site along a chromosome reduces the probability of additional COs in adjacent chromosomal regions. Thus, COs are spaced far apart along the chromosome arms. A small percentage of COs (~15%) arise independently of the ZMMs and are distinct in that they do not exhibit CO interference. It is proposed that NCOs arise via synthesis-dependent strand annealing rather than from double Holliday junctions that are the defining feature of the CO pathway (Schwacha and Kleckner, 1995; Allers and Lichten, 2001; Hunter and Kleckner, 2001; McMahill et al., 2007). Studies in the model plant *Arabidopsis thaliana* and other plant species, such as rice (*Oryza sativa*), maize (*Zea mays*), and barley (*Hordeum vulgare*), suggest that CO formation is very similar to that in budding yeast despite some differences in detail (Osman et al., 2011). The nature of the NCO in plants has not yet been determined. In fission yeast, the helicase Fml1 (Fanconi anemia complementation group M-like protein) has been shown to direct NCO formation (Lorenz et al., 2012). In *Arabidopsis*, the FANCM helicase protein plays a major role in limiting meiotic CO, suggesting a potential role in NCO formation (Crismani et al., 2012; Knoll et al., 2012). Direct analysis of NCOs and their distribution

[1] These authors contributed equally to this work.

[2] Current address: School of Biological Sciences, Adrian Building, University Road, University of Leicester, Leicester LE1 7RH, UK.

[3] Senior authors for Birmingham and Dundee, respectively.

[4] Address correspondence to c.halpin@dundee.ac.uk.

The authors responsible for distribution of materials integral to the findings presented in this article in accordance with the policy described in the Instructions for Authors (www.plantcell.org) are: Susan J. Armstrong (s.j.armstrong@bham.ac.uk) and Claire Halpin (c.halpin@dundee.ac.uk).

[W] Online version contains Web-only data.

[OPEN] Articles can be viewed online without a subscription.

www.plantcell.org/cgi/doi/10.1105/tpc.113.121269

has been difficult as they are hard to detect; however, recent sequencing approaches are beginning to yield insights (e.g., Drouaud et al., 2013; Wijnker et al., 2013).

Evidence from budding yeast indicates that the fate of individual DSBs to proceed via the CO or NCO route is designated prior to the establishment of a stable single end invasion intermediate. Imposition of this fate is dependent on the ZMMs and coordinated with the formation of the synaptonemal complex (SC), a tripartite proteinaceous structure that holds the homologs in close apposition during pachytene (Heyting, 1996; Zickler and Kleckner, 1999). The SC is comprised of two lateral elements derived from the axial elements that are established during leptotene and that organize each pair of sister chromatids into linear looped arrays conjoined at the loop bases (Zickler and Kleckner, 1999). During zygotene, the Zip1 protein forms a transverse filament that polymerizes along the aligned lateral elements to form a zipper-like structure. In budding yeast, SC formation is initiated at discrete synapsis initiation centers that are coincident with CO-designated ZMM recombination intermediates (Börner et al., 2004). Studies in *Arabidopsis* have also revealed that SC initiation sites colocalize with ZMM proteins, such as MSH4 (Higgins et al., 2004). However, the number of synapsis initiation centers appears to be greater than the eventual number of COs, suggesting an additional level of control. In budding yeast, *zip1* mutants exhibit defects in SC formation and recombination. The nature of the recombination defect is temperature dependent. At 33°C, DSBs and NCOs occur as normal, but interference-dependent COs are absent due to a failure of progression from DSBs to stable strand end invasion intermediates. At 23°C, *zip1* mutants display a different phenotype; strand end invasion and double Holliday junction intermediates are formed with a delay relative to the wild type, but there is an overall reduction in COs and a corresponding increase in NCOs. Thus, it appears that CO designation occurs, but this is not maintained, and CO fate specification is ultimately lost (Börner et al., 2004).

Previous studies in *Arabidopsis*, rice, maize, and wheat (*Triticum aestivum*) have identified plant Zip1 orthologs (Higgins et al., 2005; Wang et al., 2010; Golubovskaya et al., 2011; Khoo et al., 2012). *Arabidopsis* contains two partially redundant proteins ZYP1a and ZYP1b (collectively ZYP1), whereas rice possesses a single protein referred to as ZEP1. Rice ZEP1 exhibits 42% identity with ZYP1b and 41% identity with ZYP1a. The plant proteins exhibit little primary sequence identity with Zip1 and transverse filament proteins from other species, such as c(3)G in *Drosophila melanogaster* and Sypc1 in mouse (Page and Hawley, 2001; de Vries et al., 2005). Despite this lack of primary sequence homology, the plant proteins show structural similarity to the transverse filament proteins from other species. All comprise coiled-coil proteins with globular domains at their N and C termini (Suzuki, 1989). This is in keeping with the close ultrastructural similarity of the SC observed by electron microscopy in a wide variety of species (Zickler and Kleckner, 1999). *Arabidopsis* and rice lines lacking these transverse filament proteins through mutation or RNA interference (RNAi) knockdown fail to form SCs and exhibit defects in CO control (Higgins et al., 2005; Wang et al., 2010). In the case of *Arabidopsis*, a reduction in chiasma frequency to around 70% is observed. This is accompanied by extensive multivalent formation due to ectopic recombination possibly between chromosomal regions that have undergone segmental duplication during the evolution of this species (Higgins et al., 2005). Unexpectedly, and in contrast with *Arabidopsis* and other species, *zep1* mutants in rice are reported to exhibit an increase in chiasma frequency, with 3 to 4 times the number of COs observed on the short arm of chromosome 11 in the mutant compared with the wild type (Wang et al., 2010).

In members of the Poaceae family, such as barley, wheat, rye (*Secale cereale*), and oat (*Avena sativa*), meiotic COs predominantly occur in the distal regions of the chromosomes (Sandhu and Gill, 2002; Mayer et al., 2011). Studies indicate that this pattern is strongly influenced by the timing of recombination initiation (Higgins et al., 2012). A consequence of this is that interstitial chromosomal regions encoding an estimated 30 to 50% of the gene complement rarely recombine. This is a significant problem for plant breeding programs as it limits access to the available genetic variation and hampers both gene isolation and the introgression of new genetic traits. Since rice is a member of the Poaceae, the observation that the loss of ZEP1 led to an increase in recombination suggested a potential route to increase CO formation in the nonrecombining chromosomal regions in other cultivated members of the family, such as barley.

In this study, we used RNAi to knock down expression of *ZYP1* that encodes the barley ZEP1 homolog. Quantitative real-time PCR and immunocytochemistry confirm that transcript and protein expression has been reduced to very low levels in the transgenic barley lines; as a result, they fail to form a SC at pachytene. Surprisingly, these lines exhibit a recombination defect that contrasts starkly with that reported for rice. Rather than an increase in COs, downregulation of ZYP1 results in a dramatic reduction in CO formation that is reminiscent of that observed in *zip1* mutants of budding yeast and *Arabidopsis*.

RESULTS

Production of *ZYP1* Knockdown Barley Lines

We previously reported cloning of the full-length barley *ZYP1* cDNA (Higgins et al., 2012). Alignment of the predicted protein sequence with other plant full-length ZYP1 sequences and assembly of a phylogenetic tree (Figure 1A; Supplemental Data Set 1) reveal clear separation of the monocot and dicot sequences and confirm that the barley gene is closely related to the functionally characterized rice *ZEP1* (Wang et al., 2010). *ZYP1* expression levels determined in different organs of barley cv Golden Promise using quantitative real-time PCR (qPCR) confirmed that the transcript was highly abundant in young meiotic spikes (0.5- to 1.5-mm anthers) (Figure 1B).

An RNAi construct composed of an 800-bp fragment of the *ZYP1* cDNA in the Gateway-based hairpin vector pBRACT207 was used to generate 43 independent $ZYP1^{RNAi}$ lines in barley cv Golden Promise. Transgene integration was confirmed by PCR of the hygromycin resistance gene from plant genomic DNA. At maturity, the majority of the T0 plants showed reduced fertility compared with empty vector control plants, and some did not grow to normal height. Only plants with normal vegetative phenotypes were used for subsequent studies. The number of loci where transgenes

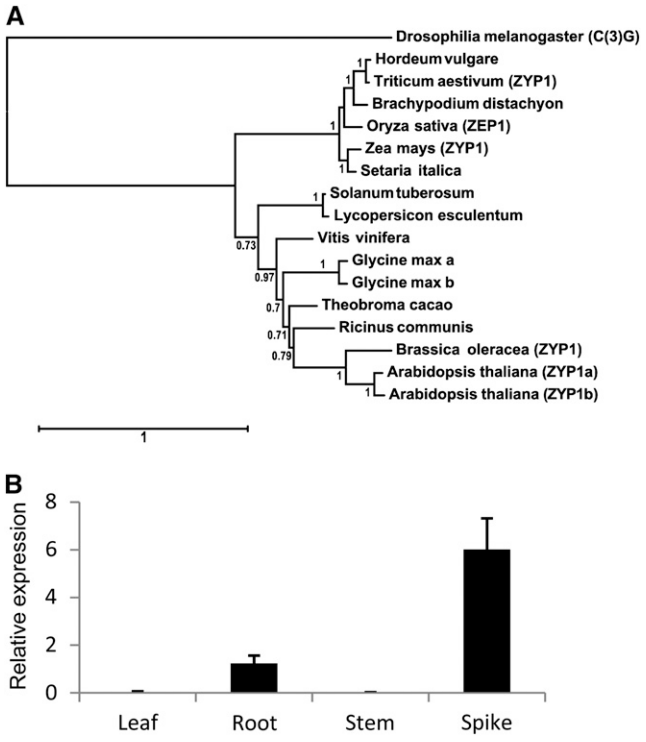

Figure 1. *ZYP1* Expression and Phylogenetic Tree.

(A) ZYP1 phylogenetic tree using full-length amino acid sequences from plants and *D. melanogaster* as the out-group. Numbers indicate statistical support, provided as posterior probabilities. The scale bar at the bottom gives the number of expected substitutions per site.

(B) *ZYP1* mRNA levels in different organs of barley cv Golden Promise were monitored using qPCR. Three samples each were collected from four plants. Error bars represent SD (n = 12).

had integrated was determined by the segregation of hygromycin resistance in germinating T1 seeds (Supplemental Table 1). In addition, a cytological analysis of 4′,6-diamidino-2-phenylindole (DAPI)–stained chromosome spreads from meiocytes of T0 plants at metaphase I was conducted to determine whether there were any chromosome abnormalities. Based on these analyses, five lines that appeared to have a single locus where a transgene (or transgenes) had inserted and no obvious chromosomal aberrations were selected for further study and production of homozygotes. Lines selected were *ZYP1^{RNAi}15*, *ZYP1^{RNAi}24*, *ZYP1^{RNAi}30*, *ZYP1^{RNAi}35*, and *ZYP1^{RNAi}43* plus two empty vector control lines. The presence of a single transgene locus in these lines was confirmed by fluorescence in situ hybridization (FISH) on meiotic prophase I chromosome spreads using the pBRACT empty vector as a probe. *ZYP1^{RNAi}* lines *15*, *24*, *30*, *35*, and *43* appeared to contain a single homozygous transgene insertion locus, whereas the empty vector line contained two transgene insertion loci (Supplemental Figure 1), and a nontransformed plant produced no signal.

Substantial reductions of *ZYP1* mRNA were evident by qPCR in the inflorescences of T1 plants of the selected *ZYP1^{RNAi}* lines (15, 24, 30, 35, and 43) compared with their segregating azygous siblings (i.e., the T1 progeny that lost the transgene through segregation) and empty vector controls (Figure 2). The lines were screened for reduced fertility as an indicator of a possible meiotic defect. Seed numbers per spike were scored for plants of each of the five selected lines and the empty vector control (Figure 3; Supplemental Figure 2). All *ZYP1^{RNAi}* transgenic plants showed a strong reduction in the number of seeds per spike compared with the control lines.

SC Formation Is Severely Affected by ZYP1 Knockdown

ZYP1 forms the transverse filaments of the SC in plants and has been identified in *Arabidopsis*, rice (known as ZEP1), maize, barley, and wheat (Higgins et al., 2005, 2012; Wang et al., 2010; Golubovskaya et al., 2011; Khoo et al., 2012). ZYP1 is initially observed in chromosome spread preparations from wild-type barley meiocytes at leptotene as foci in the subtelomeric regions (Higgins et al., 2012). These elongate to form stretches concurrent with further foci appearing in the chromosomal interstitial and proximal regions, and the stretches continue to extend and coalesce until full synapsis is achieved at pachytene (Higgins et al., 2012). In this study, the same pattern was observed by immunolocalization of ZYP1 during prophase I using the *Arabidopsis* ZYP1 antibody on the empty vector control (Figures 4A to 4E; Supplemental Figure 3A). In the *ZYP1^{RNAi}* lines, ZYP1 protein expression was significantly depleted such that none of the cells analyzed (n = 157) achieved full synapsis; nevertheless, it was also rare for there to be a complete absence of the protein (Figures 4F to 4J; Supplemental Figure 3B), consistent with the qPCR data showing residual transcript levels (Figure 2). The majority of cells had multiple foci and short stretches of ZYP1 with occasional longer stretches also observed.

To quantify the amount of polymerized ZYP1 for each cell, the total length of the stretches was measured by tracing chromosomes using the Nikon NIS-Elements software. We have previously shown that nuclei at the beginning of zygotene have a large envelope volume (i.e., the volume of all of the chromatin, as defined in Kleckner et al., 2004), which decreases as ZYP1 polymerization progresses (Higgins et al., 2012). Therefore, to accurately determine the meiotic stage of cells, it was necessary to take into account

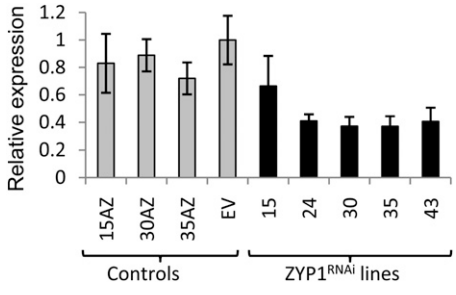

Figure 2. *ZYP1* mRNA Level in the Spikes of Five RNAi Lines.

Expression of *ZYP1* in meiotic inflorescences of five independent RNAi T1 lines (*ZYP1^{RNAi}15*, *ZYP1^{RNAi}24*, *ZYP1^{RNAi}30*, *ZYP1^{RNAi}35*, and *ZYP1^{RNAi}43*) relative to control plants (empty vector [EV]) monitored using qPCR. Error bars represent SD (n = 3 to 12, depending on the line). The *ZYP1* mRNA level in each *ZYP1^{RNAi}* line was significantly lower than in the empty vector control ($P < 0.05$). Segregating azygous (AZ) progeny lacking the transgene were available for three *ZYP1^{RNAi}* lines (15AZ, 30AZ, and 35AZ) and were included for comparison.

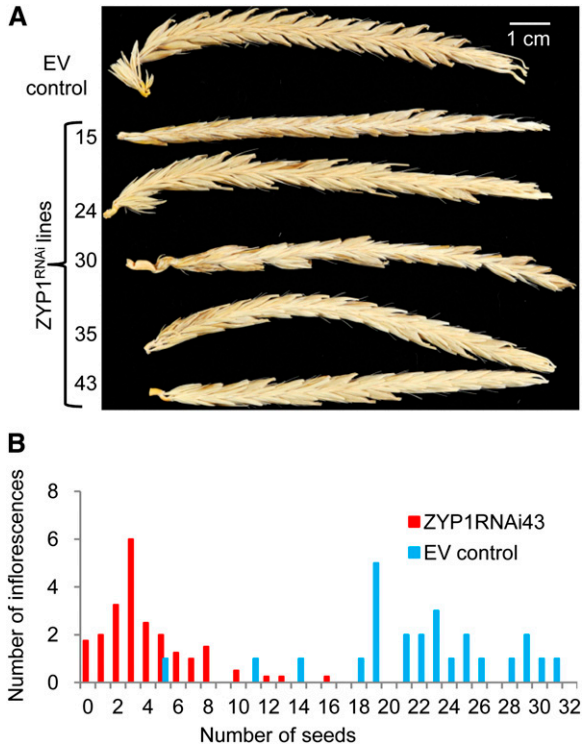

Figure 3. *ZYP1* Suppression Induces Sterility in Barley.

(A) Representative mature spikes of control (empty vector [EV]) and five different RNAi lines. Compared with the fertile EV control, all *ZYP1*^{RNAi} lines are semisterile with only a few seeds.

(B) Seed number distribution per spike of four segregating plants of *ZYP1*^{RNAi}*43* and an empty vector control plant (EV7).

nucleus size as well as ZYP1 total length. In the empty vector control, short stretches of ZYP1 were observed in nuclei with very large nuclear volumes and as these decreased, ZYP1 length increased (Figure 4K). Total ZYP1 length reached its peak at late zygotene and then decreased to pachytene, in a pattern described by a polynomial curve. At late zygotene, ZYP1 protein loading is not complete between the chromosome axes (Figures 4D and 4K), but as it reaches completion, the length of ZYP1 labeled material paradoxically reduces (Figure 4K). This is due to the chromosome axes decreasing in length between late zygotene and pachytene. Therefore, a polynomial curve was used to fit data points from total length of ZYP1 stretches in the *ZYP1*^{RNAi} lines and to compare with the peak ZYP1 polymerization in the empty vector (nuclei size = 1000 μm^2). At this peak point, total ZYP1 length in the empty vector was 566 μm compared with 13 to 95 μm in the *ZYP1*^{RNAi} lines, a reduction of 83 to 98%. Values in individual transgenic lines were 50 μm in *ZYP1*^{RNAi}*15* (8% of empty vector), 56 μm in *ZYP1*^{RNAi}*24* (10%), 28 μm in *ZYP1*^{RNAi}*30* (5%), 13 μm in *ZYP1*^{RNAi}*35* (2%), and 95 μm in *ZYP1*^{RNAi}*43* (17%).

Bivalents Are Reduced, Leading to Chromosome Nondisjunction

To gain insight into the effect of ZYP1 depletion on chiasma formation, we performed a cytological analysis on chromosome spread preparations in the transgenic lines. The empty vector control line was indistinguishable from the wild-type plant. Pachytene nuclei were commonly observed during prophase I, where the homologs were closely juxtaposed (Figure 5A). This was followed by metaphase I where seven bivalents aligned, distinguished by 5*S* and 45*S* rDNA FISH probes (Figure 5B). At metaphase II, the seven pairs of homologs had migrated to the poles and by telophase II, the sister chromatids had separated to leave four haploid cells containing seven chromosomes (Figures 5C and 5D). By contrast, pachytene nuclei were never observed in the *ZYP1*^{RNAi} lines, although many stages similar to zygotene were found (Figure 5E; Supplemental Figures 4A, 4E, 4I, and 4M). At metaphase, the number of bivalents per cell was reduced by over half from 7 (n = 60) in the empty vector control to an average of 3.13 (n = 255) in the *ZYP1*^{RNAi} lines, and many univalents were observed (Figure 5F; Supplemental Figures 4B, 4F, 4J, and 4N). This led to chromosome nondisjunction at metaphase II and telophase II (Figures 5G and 5H; Supplemental Figures 4C, 4D, 4G, 4H, 4K, 4L, 4O, and 4P).

Number of Chiasmata per Meiocyte Is Reduced, but Localization Remains Distal

There was a significant reduction in the mean number of chiasmata per cell between the empty vector (14.18 $\pm$ 0.13, n = 60) and the *ZYP1*^{RNAi} lines (3.82 $\pm$ 0.19, n = 255) ($P < 0.001$, 314 *df*), and this was consistent across all chromosomes (Supplemental Figure 5). The reduction of chiasmata varied between lines ranging from *ZYP1*^{RNAi}*35* with a mean of 1.4 $\pm$ 0.18 (n = 54) chiasmata per cell to *ZYP1*^{RNAi}*30* with 6.3 $\pm$ 0.42 (n = 53). The number of chiasmata per cell in the empty vector plant differed significantly from a Poisson distribution [$\chi_{(19)}^2$ = 107.06; $P < 0.001$], indicating a nonrandom underlying process and highlighting the existence of CO control mechanisms. However, the numerical distribution of residual chiasmata in *ZYP1*^{RNAi}*35* followed a Poisson distribution [$\chi_{(7)}^2$ = 4.73; $P > 0.10$], indicating loss of that control (Figure 6). This observation is similar to previous studies in *zmm* mutants in *Arabidopsis* and rice and consistent with a CO control defect leading to a loss of CO assurance (i.e., the obligate establishment of at least one CO per chromosome pair) (Higgins et al., 2004; Wang et al., 2012). Nevertheless, the distribution of the residual chiasmata in the *ZYP1*^{RNAi} lines remained confined to the distal regions (974/975 chiasmata observed in 255 cells) of the chromosomes similar to that in the control (785/818 chiasmata observed in 60 cells) and previously reported in the wild type (Higgins et al., 2012).

DSB Formation Appears Normal but the Recombination Pathway Is Defective

Although it is not yet possible to directly assay meiotic DSB formation in plants, immunolocalization of recombination proteins can be used to infer the number of breaks based on the number of foci observed in early prophase I. Antibodies against γH2AX, the phosphorylated form of H2AX that marks DSBs, and recombination pathway proteins including RAD51 and DMC1 have been extensively used for this purpose (Sanchez-Moran et al., 2007; Ferdous et al., 2012; Higgins et al., 2012). The number of γH2AX foci observed in chromosome spreads from meiocytes at leptotene did not differ significantly between empty vector controls and *ZYP1*^{RNAi}

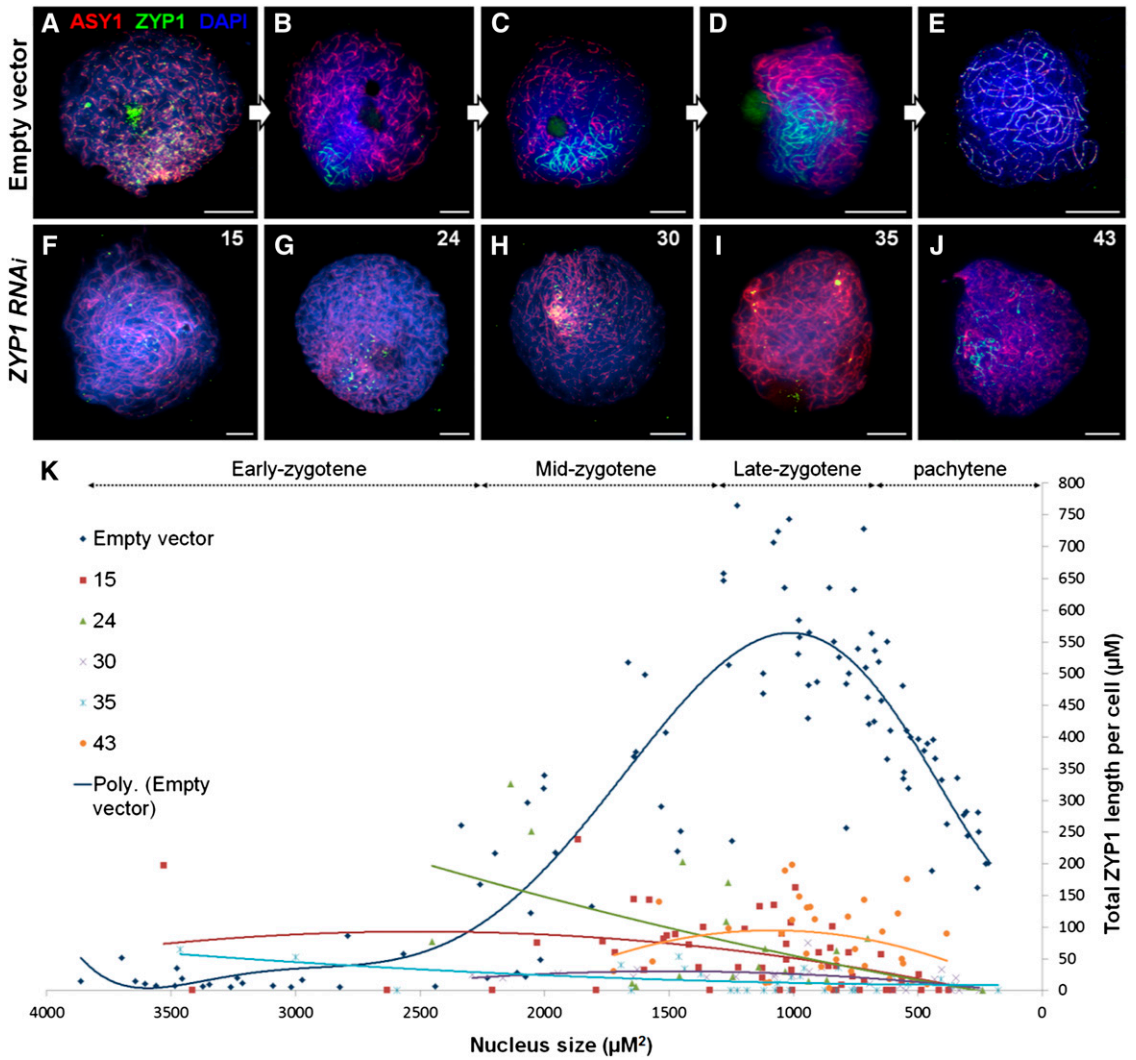

Figure 4. Quantification of ZYP1 Expression during Meiotic Prophase I.

(A) In the empty vector control, immunolocalization of ZYP1 (green) is first observed as numerous foci throughout the nucleus on the chromosome axes marked by ASY1 (red).

(B) to **(E)** During zygotene, short stretches of ZYP1 are observed that elongate until reaching full synapsis at pachytene **(E)**.

(F) to **(J)** In the *ZYP1*^{RNAi} lines (numbers shown in top right of image) the majority of nuclei contained a small number of ZYP1 foci and short stretches. Nuclei were counterstained with DAPI. Bars = 10 μm.

(K) Total ZYP1 lengths for each cell were measured by chromosome tracing and plotted against nuclei size to determine the correct stage. Polynomial curves were fitted to the data collected from the empty vector control and the numbered *ZYP1*^{RNAi} lines.

lines (Figures 7A and 7F; Supplemental Figure 6 and Supplemental Table 2). RAD51 foci counts also did not differ (Figures 7B and 7G; Supplemental Figure 7 and Supplemental Table 2). This suggests that DSB formation is unaffected in the *ZYP1*^{RNAi} lines analyzed in this study.

The meiosis-specific MutS homolog 4 (MSH4) is essential for ~85% of COs in *Arabidopsis* (Higgins et al., 2004). In barley, MSH4 localizes to the emergent chromosome axes during early leptotene as numerous foci associated with the distal chromosomal regions. As leptotene progresses, MSH4 foci increase to ~400 per nucleus distributed across the length of the mature chromosome axes, then gradually reduce such that at early zygotene around 18 to 20 foci remain (Higgins et al., 2004, 2012). In the empty vector control line, the number of MSH4 foci was indistinguishable from wild-type plants, accumulating to a maximum of 394 ± 6 (n = 10) at mid/late leptotene before reducing in number. The average number of MSH4 foci at early/mid leptotene from across the *ZYP1*^{RNAi} lines was not significantly different to the control (406 ± 18, n = 26) (P = 0.69, 35 *df*) (Figures 7C and 7H; Supplemental Figure 8 and Supplemental Table 2). However, by late leptotene, when ASY1 polymerization was complete, these had disappeared to leave a number of large MSH4 foci (45 ± 3, n = 29) that were not observed in the wild type or empty vector control lines (Figures 7D and 7I; Supplemental Figure 9 and

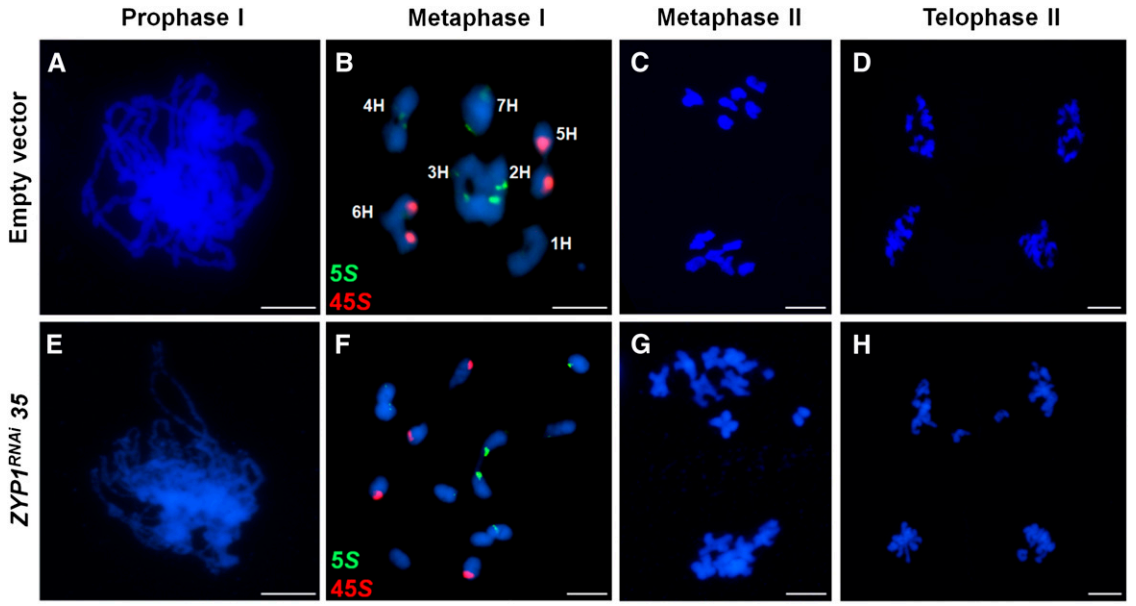

Figure 5. A Cytological Analysis of Meiotic Chromosomes in *ZYP1*^{RNAi}.

In the empty vector control, chromosomes are in close alignment during prophase I **(A)**. At metaphase I, bivalents of the seven barley chromosomes, 1H to 7H, can be distinguished with 5*S* (green) and 45*S* (red) ribosomal DNA fluorescence in situ hybridization probes **(B)**. At metaphase II, the homologs have separated so there are seven chromosomes at each pole **(C)**. At telophase II, the sister chromatids have separated to give four haploid cells each with seven chromosomes **(D)**. In a representative *ZYP1*^{RNAi} line (35), chromosomes never become fully aligned during prophase I **(E)**. At metaphase I, a large number of univalents are observed with occasional bivalents **(F)**. Reduced chiasmata at metaphase I led to chromosome nondisjunction at metaphase II **(G)** and telophase II **(H)**. Nuclei were stained with DAPI. Bars = 10 μm.

Supplemental Table 2). They persisted to zygotene when the short stretches of SC that can still form in the *ZYP1*^{RNAi} lines are present but had disappeared by late prophase I.

The MutL homolog 3 (MLH3) is a meiosis-specific protein required to form normal levels of interference-sensitive COs in *Arabidopsis* (Jackson et al., 2006). In barley, it marks late recombination nodules, the future sites of interference-dependent COs (Phillips et al., 2013). The number of MLH3 foci during prophase I in the empty vector control line (15 ± 2.4, $n = 10$) was significantly greater ($P < 0.001$, 51 *df*) than the number of pooled MLH3 foci from the *ZYP1*^{RNAi} lines (2 ± 0.2, $n = 42$) (Figures 7E and 7J; Supplemental Figure 10 and Supplemental Table 2). MLH3 foci numbers ranged from 11 to 18 in the empty vector control and 0 to 6 in the *ZYP1*^{RNAi} lines. The numerical distribution of MLH3 foci per meiocyte did not differ significantly from a Poisson distribution [$\chi_{(6)}^2 = 8.13$; $P > 0.05$] consistent with a breakdown in CO control leading to a random loss of Class I, interference-dependent COs (Jackson et al., 2006). Collectively, these data suggest that, while DSBs appear to occur normally in *ZYP1*^{RNAi} plants, aspects of the later stages of the recombination pathway are compromised leading to a reduction in CO formation but not DSB repair.

Meiotic Progression Is Delayed by ZYP1 Depletion

In *Arabidopsis,* depletion of the ZYP1 protein perturbs the meiotic program, leading to a delay during prophase I (Higgins et al., 2005). Therefore, if completion of chromosome synapsis is acting as a checkpoint during prophase I, depleting the ZYP1 protein in barley may lead to a delay and alter meiotic progression. To investigate this possibility, we performed a meiotic time course using bromodeoxyuridine (BrdU) using the empty vector control and *ZYP1*^{RNAi}*43* plants. In the empty vector

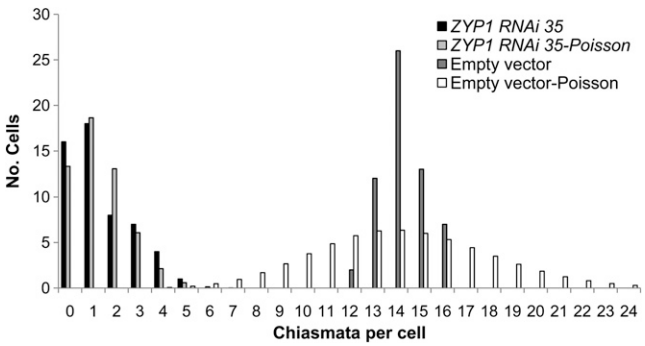

Figure 6. Chiasma Frequency in *ZYP1*^{RNAi}*35* and the Empty Vector Control Compared with the Predicted Poisson Distribution.

Metaphase I chromosomes stained with DAPI and labeled with 5*S* and 45*S* rDNA FISH probes were scored for chiasmata in *ZYP1*^{RNAi}*35* (black) and the empty vector control (dark gray). The chiasma frequency in the control does not fit a Poisson distribution (white), whereas chiasmata in *ZYP1*^{RNAi}*35* do not significantly differ from a Poisson distribution (light gray).

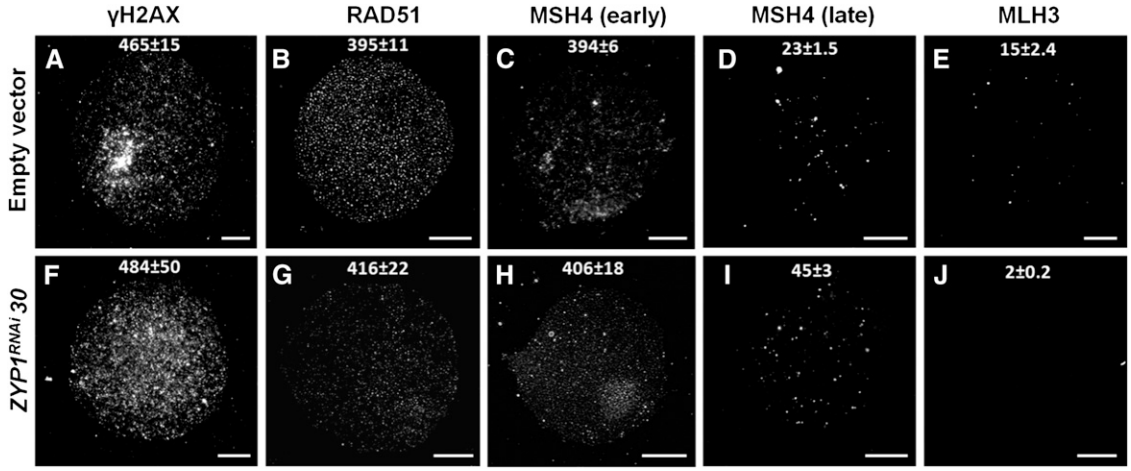

Figure 7. Immunolocalization and Quantification of Recombination Protein Loading in *ZYP1*^{RNAi}*30* and the Empty Vector Control.

Markers for early meiotic recombination events, such as γH2AX, RAD51 and MSH4, are indistinguishable between *ZYP1*^{RNAi}*30* (**[F]** to **[H]**) and the empty vector control (**[A]** to **[C]**). In *ZYP1*^{RNAi}*30*, later events are affected as there is an increased number of large MSH4 foci compared with the control (**[I]** compared with **[D]**) and MLH3 foci are reduced (**[J]** compared with **[E]**). Numbers represent average number of foci labeled per cell ± SE (*n* = 5 to 10). Full quantification data are shown in Supplemental Table 2, and exemplar images for all lines are in Supplemental Figures 5 to 9. Bars = 10 μm.

control, the first labeled tetrads were identified after 43 h (Figure 8A). One *ZYP1*^{RNAi}*43* plant progressed to first labeled tetrads after 55 h, an approximate 12-h delay (Figures 8B to 8F), while cells of four other plants remained in prophase I. Thus, reduction of ZYP1 expression causes a substantial delay in prophase I progression.

DISCUSSION

We identified and cloned barley *ZYP1* and suppressed its expression to very low levels using a constitutively expressed RNAi construct to evaluate its role in meiotic CO formation. Our results suggest an essential role for ZYP1 in ensuring that CO-designated DSB sites progress to form late recombination intermediates and full COs. Without ZYP1, CO numbers are dramatically reduced. In this respect, barley ZYP1 appears to function similarly to ZIP1/ZYP1 in yeast and *Arabidopsis*, respectively, and has an opposite effect on CO number to that reported for its ortholog, ZEP1, in rice, another member of the Poaceae.

ZYP1 Protein Is Critical for Synapsis and Timely Prophase I Progression in Barley

Prophase I meiocytes of our *ZYP1*^{RNAi} transgenic lines had greatly reduced stretches of SC ranging from 2 to 17% of that of the empty vector control, consistent with ZYP1 forming the transverse filaments of the SC. Although fertility was dramatically reduced, all transgenic lines produced some seed, and this is likely due to the fact that occasional meiocytes retained longer tracts of SC and more residual chiasmata than the average. A minimum delay of 12 h in prophase I was observed in the *ZYP1*^{RNAi}*43* line, which was the line with most residual ZYP1 protein. This is consistent with data from *Arabidopsis* where a 6- to 20-h delay was seen in ZYP1 T-DNA mutants or RNAi knockdown plants (Higgins et al., 2005). Based on studies in budding yeast and mouse meiotic mutants, it has been proposed that such delays may be associated with the monitoring of prophase I by a surveillance system that ensures correct regulatory responses to meiotic defects (Hunt and Hassold, 2002; Börner et al., 2004; Barchi et al., 2005). The prophase I delay observed in barley in response to reduced ZYP1, taken in conjunction with the previous results in *Arabidopsis*, provides evidence consistent with a prophase I surveillance system in all plants.

ZYP1 Is Required to Implement CO Formation in Barley

The early stages of prophase I appear unaltered in the *ZYP1*^{RNAi} lines. This is consistent with data from barley and maize suggesting that a role demonstrated for budding yeast Zip1 in centromere coupling during early meiosis (Tsubouchi and Roeder, 2005) is not conserved in these grasses, where ZYP1 is not detected in centromeres at leptotene (Phillips et al., 2012; Zhang et al., 2013). Our immunolocalization studies using anti-γH2AX and anti-RAD51 antibodies suggest that DSB formation and the initial stages of recombination proceed as normal in the *ZYP1*^{RNAi} lines. MSH4 localization also appears to be normal with ~400 foci up to mid leptotene but then, instead of a gradual transition to ~20 foci in zygotene, there is precocious loss in the *ZYP1*^{RNAi} lines such that the number of foci decreases from wild-type levels at mid leptotene down to ~40 foci at late leptotene. Morphologically these foci appear larger than normal, suggesting that they correspond to protein accumulations. However, they are consistent in size and number and are axis associated as they colocalize with ASY1, suggesting that they are not the protein polycomplexes that are observed in some meiotic mutants (Chen et al., 2011). It is tempting to speculate that they may correspond to sites of recombination intermediates that have somehow stalled or are progressing more slowly due to the reduced levels of ZYP1. One possibility is that they mark synapsis initiation sites. The defect in MSH4 localization is accompanied by a reduction in

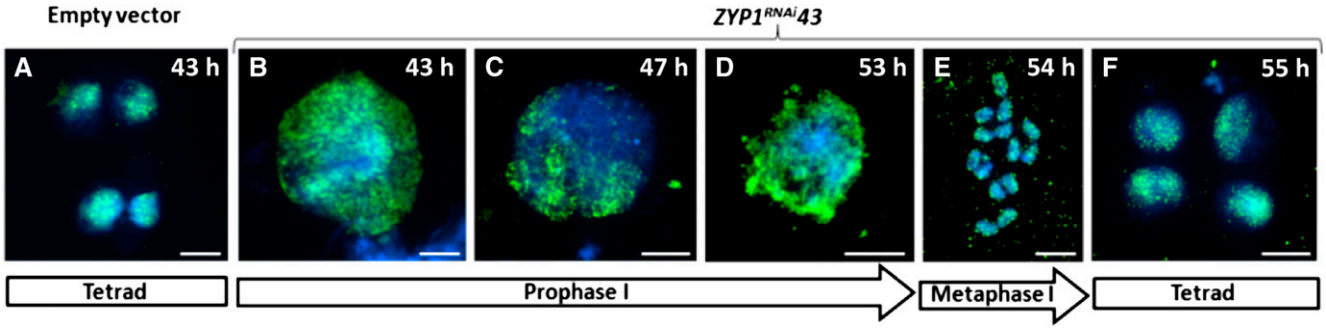

Figure 8. Time-Course Determination of the Effect of *ZYP1*^{RNAi} on the Duration of Meiosis.

BrdU (green) was incorporated into DNA during premeiotic S-phase, and samples were fixed at various time intervals. In the empty vector control, BrdU-labeled tetrads were observed at 43 h **(A)**, whereas the furthest stage reached in *ZYP1*^{RNAi}*43* at 43 h was early prophase **(B)**. This delay in meiosis progression in *ZYP1*^{RNAi}*43* continued at 47 h **(C)** and 53 h **(D)** until labeled metaphase I nuclei were detected at 54 h **(E)**. Labeled tetrads were finally observed only at 55 h **(F)** in *ZYP1*^{RNAii}*43*. Bars = 10 μm.

the number of MLH3 foci. Biochemical studies using purified human MSH4/MSH5 indicate that the complex binds and stabilizes proto-Holliday junctions following single-end invasion (Snowden et al., 2004). As it appears that this function is conserved in other species including plants (Wang et al., 2012), the destabilization of MSH4 localization in the *ZYP1*^{RNAi} lines would suggest a defect in the formation of late recombination intermediates.

The meiotic phenotype of the barley *ZYP1*^{RNAi} lines indicates that, like Zip1 in budding yeast, ZYP1 is essential for normal levels of CO formation. A reduction in mean chiasma frequency to 3.82 per meiocyte was observed for the lines as a whole, ~10 to 44% of the empty vector control. Based on our observations, we propose that ZYP1 is recruited to early recombination pathway intermediates. In the *ZYP1*^{RNAi} lines, CO designation still occurs, possibly inefficiently, but due to a reduced level of ZYP1 protein, CO imposition is aberrant. As a result, CO formation is reduced with a proportion of CO-designated intermediates reverting to a non-CO fate or being repaired via some other route such as intersister chromatid recombination.

In budding yeast, it is proposed that the ZMM proteins ensure that CO-designated recombination intermediates and structural components of the meiotic chromosomes are correctly coupled, thereby allowing normal progression of recombination (Börner et al., 2004). At designated CO sites, the formation of stable single-end invasion intermediates is accompanied by SC nucleation to produce a recombination complex. In the absence of Zip1 or other ZMMs, CO formation is impeded in a temperature-differential manner (see Introduction) (Börner et al., 2004). Our data are consistent with ZYP1 performing a similar role in the barley recombination pathway.

Residual Chiasmata in the *ZYP1*^{RNAi} Lines Are Strongly Localized

The number of chiasmata per nucleus in EV control plants was significantly more overdistributed around a mean of 14 (i.e., two per chromosome) than a Poisson distribution would predict. This nonrandom control was lost in the *ZYP1*^{RNAi} lines where the number of residual chiasmata/COs per nucleus fitted a Poisson distribution around a mean of 1.4 ± 0.18 (n = 54), suggesting a random process. These data clearly indicate that ZYP1 plays an important role in CO control. However, the position of residual COs in *ZYP1*^{RNAi} lines was highly regulated with virtually all occurring in the distal regions of the chromosomes. This is similar to what is normally found in wild-type barley where interstitial chiasmata are generally rare (Higgins et al., 2012). In the control lines analyzed here, they accounted for only 0.04% of the total chiasmata. In the *ZYP1*^{RNAi} lines, the mean frequency of chiasmata was 27% of the control, but there was a near complete absence of interstitial chiasmata, a proportionally greater effect than on distal chiasmata. This may simply reflect the fact that the initiation of recombination and synapsis in barley occurs in subtelomeric DNA in advance of interstitial events (Higgins et al., 2012). When ZYP1 protein is limiting, it may be preferentially recruited to distal regions, further restricting any possible recruitment to interstitial sites. It is conceivable that other factors may also influence this. For example, the chromosome bouquet that forms at early zygotene, clustering telomeres on the nuclear membrane (Scherthan, 2001), may promote the stability of interhomolog recombination interactions that are close to the telomeric region.

Reduced SC Transverse Filament Protein Produces Different Effects in Closely Related Grass Species

The proteins that form the transverse element of the SC have been identified in a number of species; these include Zip1 in budding yeast, SYCP1 in mouse, C(3)G in *D. melanogaster*, and SYP-1/SYP-2 in *Caenorhabditis elegans*. In all cases, mutation of the corresponding genes results in a failure to form SC together with a reduction in CO formation (Sym et al., 1993; Heyting, 1996; Page and Hawley, 2001; MacQueen et al., 2002). Interestingly, in *SYP-1* RNAi *C. elegans* where sufficient SYP-1 is retained to permit assembly of the SC, a reduction is observed in the distance over which interference operates, and the number of COs is increased (Libuda et al., 2013). This is likely a consequence of the distinct way that *C. elegans* controls CO designation, which takes place after the assembly of the SC. By contrast, in budding yeast, CO designation occurs before stable

single end invasions (i.e., before SC formation begins), although ZYP1 is subsequently required to implement the designated CO fate (Hunter and Kleckner, 2001; Börner et al., 2004). This seems to be the case in plants also; in *Arabidopsis* T-DNA lines lacking either one of two duplicated *ZYP1* genes, there is a modest 10% reduction in chiasma frequency, whereas *Arabidopsis ZYP1*^{RNAi} knockdown lines display a 30% chiasma reduction (Higgins et al., 2005). Most of the remaining *Arabidopsis* events involve ectopic recombination very likely between duplicated regions located on nonhomologous chromosomes.

Surprisingly, and in contrast with other species, a study in rice has reported a substantial increase in recombination in mutants of the *ZYP1* ortholog, *ZEP1* (Wang et al., 2010), although the CO sites were not immunologically validated as they had been in the *C. elegans* work. Nevertheless, this hyperrecombination phenotype prompted our current study as it suggested a potential route to breaking up recombinationally silent regions within the chromosomes of closely related cereals by downregulation of *ZYP1/ZEP1.* However, our data clearly demonstrate that in barley, as in all other species analyzed to date including *Arabidopsis*, severe ZYP1 depletion dramatically reduces COs. An explanation for this difference between the closely related barley and rice may lie in the fact that some of the stronger alleles in the rice work expressed ZEP1 truncated protein (Wang et al., 2010). Moreover, since robust markers for interference-dependent CO sites were not used in the rice study, it remains unknown whether these additional COs were interference dependent and/or interference independent. It is possible that the additional rice COs arose via a pathway that does not require the posited recombination-promoting function of ZEP1 during the early stages of recombination. Nevertheless, the possibility remains that multiple layers of CO control that make varying levels of relative contributions in different organisms, as suggested in reconciliation of the differences between *C. elegans* and yeast (Libuda et al., 2013), might also apply between related plant species. In summary, our study provides further evidence that functional coupling of the recombination machinery with the structural components that organize the chromosomes during prophase I is essential for the controlled formation of COs during meiosis in plants, as in other organisms.

METHODS

Plant Material

Barley (*Hordeum vulgare* cv Golden Promise) was grown to maturity in compost in a standard heated greenhouse at 22°C under 16-h photoperiod where supplementary lighting was provided by high-pressure sodium vapor lamps (Powertone SON-T AGRO 400W; Philips Electronic UK). Pollen mother cells were harvested from the inflorescences and leaf samples taken for genomic DNA extraction.

Multiple Alignment and Phylogenetic Analysis

The plant genomes platform Plaza 2.5 (http://bioinformatics.psb.ugent.be/plaza/; Van Bel et al., 2012) was searched with *Arabidopsis thaliana* ZYP1a. The plant ZYP1 amino acid sequences were aligned using the National Center for Biotechnology Information multiple protein alignment tool (http://www.ncbi.nlm.nih.gov/tools/cobalt/cobalt.cgi?link_loc=BlastHomeAd), and the full-length sequences were selected to construct the phylogenetic tree using *Drosophila melanogaster* sequence as the out-group. Selected protein sequences were aligned again using MUSCLE 3.7 and the alignment refined using Gblocks 0.91b using the pipeline of software tools available within www.phylogeny.fr (Dereeper et al., 2008). The parameters used for MUSCLE 3.7 were the default when configured for highest accuracy and for Gblocks were: minimum length of a block after gap cleaning= 10; no gap positions were allowed in the final alignment; all segments with contiguous nonconserved positions bigger than eight were rejected; and minimum number of sequences for a flank position = 85%. Phylogeny was then constructed within the TOPALi interface (Milne et al., 2009) with JTT+G as the substitution model. This model was then used to estimate a Bayesian phylogenetic tree using MrBayes v3.1.1 (Ronquist and Huelsenbeck, 2003) launched from TOPALi. The Bayesian analysis settings were two runs of 625,000 generations and a 20% burn-in with trees sampled every 10 generations. The posterior probabilities higher than 70% show support for each cluster. The alignments on which the phylogenetic tree is based are provided in Supplemental Data Set 1.

Zyp1-RNAi Construct and Transgenic Lines

A 3′-end fragment of 800 bp was amplified by PCR using two ZYP1-specific Gateway primers attB1-*HvZYP1* and attB2-*HvZYP1* (Supplemental Table 3) and the FL-*HvZYP1* plasmid DNA as template. The obtained PCR fragment was cloned into the entry vector pDONR207 using BP clonase II (Invitrogen). The resulting entry clone was used to transfer the fragment into the RNAi destination vector pBract207 (John Innes Centre) using LR Clonase (Invitrogen). The final construct where the RNAi cassette is under the transcriptional control of the constitutive *ZmUbiquitin* promoter was transferred into *Agrobacterium tumefaciens* AGL1 containing the helper plasmid pSOUP. Barley cv Golden Promise transformation was performed by the FunGen Group at The James Hutton Institute using immature embryos (Harwood et al., 2009).

Screening of Transgenic ZYP1-RNAi Lines

The T0 transgenic lines were grown to maturity and T1 seed number per tiller scored. Transgene segregation rate was determined by the root assay described by Jacobsen et al. (2006). Twenty seeds per line were germinated on solid agar (0.5% phytogel) in the presence of 100 μg/mL of hygromycin. The resistant transgenic seedlings and their segregating sensitive azygotes were scored to estimate the number of the transgene loci in each line. Based on preliminary DAPI staining of nuclei and preliminary fertility estimates from seed numbers, five semisterile lines (15, 24, 30, 35, and 43) were selected. For these, T1 seeds were germinated without hygromycin selection and grown to maturity for further analysis. The presence or absence of the transgene construct in these plants was determined by PCR using their genomic DNA and hygromycin gene-specific primers (Supplemental Table 3).

Determination of ZYP1 Expression Using qPCR

Three to five plants were grown for each selected RNAi line, empty vector control, and untransformed barley Golden Promise cultivar, and three samples per plant were collected for RNA extraction. Total RNA was extracted from leaf, root, stem, and young inflorescences (1.0 to 1.5 cm length) using TRI reagent (Sigma-Aldrich), treated with RNase-Free DNase (catalog number 79254; Qiagen), and then cleaned with RNeasy Mini Spin Columns (catalog number 74104; Qiagen). Purified RNA (2 μg) was used to make the first-strand cDNA using Superscript Vilo cDNA synthesis kit (Invitrogen). qPCR was performed using the StepOnePlus Real-time PCR system machine from Applied Biosystems and FastStart Universal Probe Master

(ROX) from Roche. qPCR was performed using Hv-*ZYP1*–specific primers Hv-*ZYP1L* and Hv-*ZYP1R* and their corresponding Roche Universal ProbeLibrary probe number 65 (catalog number 04688643001). The barley SKP1-specific (S-phase kinase-associated protein 1; accession number AK249865) primers SKP1L and SKP1R were used for internal reference in the presence of Roche Universal ProbeLibrary probe number 71 (catalog number 04688945001) (see Supplemental Table 3 for oligonucleotide list). The qPCR results were analyzed using StepOnePlus software V2.2.2. ANOVA was performed using the log of the relative expression value plus one in order to ensure that model assumptions were met. A significant difference [$F(8,63) = 72.79$, $P < 0.001$] was found between lines. An LSD at the 5% level was used to compare *ZYP1*^{RNAi} lines and their corresponding azygotes to the empty vector control.

Cytological Procedures

PMCs were examined by light microscopy after staining with DAPI, and chiasmata were recorded after FISH with 5*S* (pTa794) and 45*S* (pTa71) probes to identify individual bivalents (Leitch and Heslop-Harrison, 1993; Taketa et al., 1999; Sanchez-Moran et al., 2001). Immunolocalization and other cytological techniques were performed according to Higgins (2013). Antibodies were used at a concentration of 1:200 including At-ASY1 rat, At-ZYP1 rat, γH2AX rabbit (Millipore), At-RAD51 rabbit, At-MSH4 rabbit, and Hv-MLH3 rabbit (Phillips et al., 2013). For the cytological time course, 10 mM BrdU (0.5 mL) was injected into barley influorescences, which were then fixed in 3:1 ethanol:acetic acid at various time points and detected with BrdU labeling and detection kit I (Roche Diagnostics), as in Higgins (2013).

Microscopy

Fluorescence microscopy was performed using a Nikon Eclipse 90i microscope. NIS-elements software (Nikon) was used to record numbers of foci and trace chromosomes and to determine nucleus size. Statistical analysis was performed using Minitab and one-way ANOVA. Numbers after ± are SE.

Accession Numbers

Sequence data from this article used for the phylogenetic tree in Figure 1 can be found in the GenBank/EMBL data libraries under the following accession numbers: barley (AFP73614), *D. melanogaster* (NP_650490), wheat (*Triticum aestivum*; AFD04131), *Arabidopsis* (AT1G22260 and AT1G22275), *Brachypodium distachyon* (XP_003579875), *Theobroma cacao* (EOY16005), tomato (*Solanum lycopersicum*; XP_004238527.1), *Ricinus communis* (XP_002513917), grape (*Vitus vinifera*; XP_003634472.1), *Brassica oleracea* (ABO69625.1), potato (*Solanum tuberosum*; XP_006364852.1), rice (*Oryza sativa*; ADD69817.1), maize (*Zea mays*; NP_001182397.1), and *Setaria italica* (XP_004975811.1). Sequence data also are available at Ensembl: soybean (*Glycine max*; GLYMA13G01840 and GLYMA14G34810).

Supplemental Data

The following materials are available in the online version of this article.

Supplemental Figure 1. Determining the Number of T-DNA Inserts in *ZYP1RNAi* Lines Using Fluorescence in Situ Hybridization with pBRACT Probe on Meiotic Prophase I Nuclei.

Supplemental Figure 2. Hv-*ZYP1* Suppression Induces Sterility in Barley.

Supplemental Figure 3. Unmerged Images from Figure 4 of ZYP1 (Green) and ASY1 (Red) of Prophase I in Empty Vector Control Nuclei and of Prophase I in *ZYP1RNAi* Nuclei.

Supplemental Figure 4. A Cytological Analysis of Meiotic Chromosomes in *ZYP1RNAi* Lines That Were Not Shown in Figure 5.

Supplemental Figure 5. The Numbers of Chiasmata in Individual Chromosomes Are Differentially Affected in the *ZYP1RNAi* Lines.

Supplemental Figure 6. Immunolocalization of γH2AX in the Empty Vector Control and *ZYP1RNAi* Lines.

Supplemental Figure 7. Immunolocalization of RAD51 in the Empty Vector Control and Selected *ZYP1RNAi* Lines.

Supplemental Figure 8. Immunolocalization of MSH4 (Early Leptotene) in the Empty Vector Control and *ZYP1RNAi* Lines.

Supplemental Figure 9. Immunolocalization of MSH4 (Late Leptotene) in the Empty Vector Control and *ZYP1RNAi* Lines.

Supplemental Figure 10. Immunolocalization of MLH3 in the Empty Vector Control and *ZYP1RNAi* Lines.

Supplemental Table 1. Segregation of Hygromycin Resistance in the T1 Seed of *ZYP1RNAi* Lines and Empty Vector Control Line (EV) When Seeds Were Germinated on Hygromycin-Containing Medium.

Supplemental Table 2. Quantification of Recombination Protein Loading in the Empty Vector Control and *ZYP1RNAi* Lines.

Supplemental Table 3. Oligonucleotides Used in This Study.

Supplemental Data Set 1. Multiple Sequence Alignment on Which the Phylogenetic Tree in Figure 1 Is Based.

ACKNOWLEDGMENTS

This work was funded by Biotechnology and Biological Science Research Council Grants BB/F020872/1 and BB/F019351/1. I.C. was funded by European Community Grant FP7 222883. We thank Miriam Schreiber for help with phylogenetic analysis.

AUTHOR CONTRIBUTIONS

C.H., F.C.H.F., R.W., and S.J.A. designed the research. A.B., J.D.H., S.V., R.M.P., and L.R. performed the research. J.S. produced the transgenic plants. H.O. performed statistical analysis. J.D.H., F.C.H.F., S.J.A., I.C., A.B., and C.H. wrote the article.

Received November 27, 2013; revised January 17, 2014; accepted February 2, 2014; published February 21, 2014.

REFERENCES

Allers, T., and Lichten, M. (2001). Differential timing and control of noncrossover and crossover recombination during meiosis. Cell **106:** 47–57.

Barchi, M., Mahadevaiah, S., Di Giacomo, M., Baudat, F., de Rooij, D.G., Burgoyne, P.S., Jasin, M., and Keeney, S. (2005). Surveillance of different recombination defects in mouse spermatocytes yields distinct responses despite elimination at an identical developmental stage. Mol. Cell. Biol. **25:** 7203–7215.

Börner, G.V., Kleckner, N., and Hunter, N. (2004). Crossover/noncrossover differentiation, synaptonemal complex formation, and regulatory surveillance at the leptotene/zygotene transition of meiosis. Cell **117:** 29–45.

Chen, Z., Higgins, J.D., Hui, J.T.L., Li, J., Franklin, F.C.H., and Berger, F. (2011). Retinoblastoma protein is essential for early meiotic events in *Arabidopsis.* EMBO J. **30:** 744–755.

Cnudde, F., and Gerats, T. (2005). Meiosis: Inducing variation by reduction. Plant Biol. (Stuttg.) **7:** 321–341.

Crismani, W., Girard, C., Froger, N., Pradillo, M., Santos, J.L., Chelysheva, L., Copenhaver, G.P., Horlow, C., and Mercier, R. (2012). FANCM limits meiotic crossovers. Science **336:** 1588–1590.

Dereeper, A., Guignon, V., Blanc, G., Audic, S., Buffet, S., Chevenet, F., Dufayard, J.F., Guindon, S., Lefort, V., Lescot, M., Claverie, J.M., and Gascuel, O. (2008). Phylogeny.fr: robust phylogenetic analysis for the non-specialist. Nucleic Acids Res. **36:** W465–W469.

de Vries, F.A.T., de Boer, E., van den Bosch, M., Baarends, W.M., Ooms, M., Yuan, L., Liu, J.-G., van Zeeland, A.A., Heyting, C., and Pastink, A. (2005). Mouse Sycp1 functions in synaptonemal complex assembly, meiotic recombination, and XY body formation. Genes Dev. **19:** 1376–1389.

Drouaud, J., Khademian, H., Giraut, L., Zanni, V., Bellalou, S., Henderson, I.R., Falque, M., and Mézard, C. (2013). Contrasted patterns of crossover and non-crossover at *Arabidopsis thaliana* meiotic recombination hotspots. PLoS Genet. **9:** e1003922.

Ferdous, M., Higgins, J.D., Osman, K., Lambing, C., Roitinger, E., Mechtler, K., Armstrong, S.J., Perry, R., Pradillo, M., Cuñado, N., and Franklin, F.C.H. (2012). Inter-homolog crossing-over and synapsis in *Arabidopsis* meiosis are dependent on the chromosome axis protein AtASY3. PLoS Genet. **8:** e1002507.

Grelon, M., Vezon, D., Gendrot, G., and Pelletier, G. (2001). AtSPO11-1 is necessary for efficient meiotic recombination in plants. EMBO J. **20:** 589–600.

Golubovskaya, I.N., Wang, C.J.R., Timofejeva, L., and Cande, W.Z. (2011). Maize meiotic mutants with improper or non-homologous synapsis due to problems in pairing or synaptonemal complex formation. J. Exp. Bot. **62:** 1533–1544.

Hartung, F., Wurz-Wildersinn, R., Fuchs, J., Schubert, I., Suer, S., and Puchta, H. (2007). The catalytically active tyrosine residues of both SPO11-1 and SPO11-2 are required for meiotic double-strand break induction in *Arabidopsis*. Plant Cell **19:** 3090–3099.

Harwood, W.A., Bartlett, J.G., Alves, S.C., Perry, M., Smedley, M.A., Leyland, N., and Snape, J.W. (2009). Barley transformation using Agrobacterium-mediated techniques. Methods Mol. Biol. **478:** 137–147.

Heyting, C. (1996). Synaptonemal complexes: Structure and function. Curr. Opin. Cell Biol. **8:** 389–396.

Higgins, J.D. (2013). Analyzing meiosis in barley. Methods Mol. Biol. **990:** 135–144.

Higgins, J.D., Armstrong, S.J., Franklin, F.C.H., and Jones, G.H. (2004). The *Arabidopsis* MutS homolog AtMSH4 functions at an early step in recombination: evidence for two classes of recombination in *Arabidopsis*. Genes Dev. **18:** 2557–2570.

Higgins, J.D., Perry, R.M., Barakate, A., Ramsay, L., Waugh, R., Halpin, C., Armstrong, S.J., and Franklin, F.C. (2012). Spatiotemporal asymmetry of the meiotic program underlies the predominantly distal distribution of meiotic crossovers in barley. Plant Cell **24:** 4096–4109.

Higgins, J.D., Sanchez-Moran, E., Armstrong, S.J., Jones, G.H., and Franklin, F.C.H. (2005). The *Arabidopsis* synaptonemal complex protein ZYP1 is required for chromosome synapsis and normal fidelity of crossing over. Genes Dev. **19:** 2488–2500.

Hunt, P.A., and Hassold, T.J. (2002). Sex matters in meiosis. Science **296:** 2181–2183.

Hunter, N., and Kleckner, N. (2001). The single-end invasion: an asymmetric intermediate at the double-strand break to double-holliday junction transition of meiotic recombination. Cell **106:** 59–70.

Jackson, N., Sanchez-Moran, E., Buckling, E., Armstrong, S.J., Jones, G.H., and Franklin, F.C.H. (2006). Reduced meiotic crossovers and delayed prophase I progression in AtMLH3-deficient Arabidopsis. EMBO J. **25:** 1315–1323.

Jacobsen, J., Venables, I., Wang, M.B., Matthews, M., Ayliffe, M., and Gubler, F. (2006). Barley (*Hordeum vulgare* L.). In Agrobacterium Protocols, K. Wang, ed (Totowa, NJ: Humana Press), pp. 171–184.

Keeney, S., Giroux, C.N., and Kleckner, N. (1997). Meiosis-specific DNA double-strand breaks are catalyzed by Spo11, a member of a widely conserved protein family. Cell **88:** 375–384.

Khoo, K.H.P., Able, A.J., and Able, J.A. (2012). The isolation and characterisation of the wheat molecular ZIPper I homologue, TaZYP1. BMC Res. Notes **5:** 106.

Kleckner, N., Zickler, D., Jones, G.H., Dekker, J., Padmore, R., Henle, J., and Hutchinson, J. (2004). A mechanical basis for chromosome function. Proc. Natl. Acad. Sci. USA **101:** 12592–12597.

Knoll, A., Higgins, J.D., Seeliger, K., Reha, S.J., Dangel, N.J., Bauknecht, M., Schröpfer, S., Franklin, F.C., and Puchta, H. (2012). The Fanconi anemia ortholog FANCM ensures ordered homologous recombination in both somatic and meiotic cells in *Arabidopsis*. Plant Cell **24:** 1448–1464.

Leitch, I.J., and Heslop-Harrison, J.S. (1993). Physical mapping of four sites of 5S rDNA sequences and one site of the α-amylase-2 gene in barley (*Hordeum vulgare*). Genome **36:** 517–523.

Libuda, D.E., Uzawa, S., Meyer, B.J., and Villeneuve, A.M. (2013). Meiotic chromosome structures constrain and respond to designation of crossover sites. Nature **502:** 703–706.

Lorenz, A., Osman, F., Sun, W., Nandi, S., Steinacher, R., and Whitby, M.C. (2012). The fission yeast FANCM ortholog directs non-crossover recombination during meiosis. Science **336:** 1585–1588.

Lynn, A., Soucek, R., and Börner, G.V. (2007). ZMM proteins during meiosis: Crossover artists at work. Chromosome Res. **15:** 591–605.

MacQueen, A.J., Colaiácovo, M.P., McDonald, K., and Villeneuve, A.M. (2002). Synapsis-dependent and -independent mechanisms stabilize homolog pairing during meiotic prophase in *C. elegans*. Genes Dev. **16:** 2428–2442.

Mayer, K.F., et al. (2011). Unlocking the barley genome by chromosomal and comparative genomics. Plant Cell **23:** 1249–1263.

McMahill, M.S., Sham, C.W., and Bishop, D.K. (2007). Synthesis-dependent strand annealing in meiosis. PLoS Biol. **5:** e299.

Milne, I., Lindner, D., Bayer, M., Husmeier, D., McGuire, G., Marshall, D.F., and Wright, F. (2009). TOPALi v2: A rich graphical interface for evolutionary analyses of multiple alignments on HPC clusters and multi-core desktops. Bioinformatics **25:** 126–127.

Osman, K., Higgins, J.D., Sanchez-Moran, E., Armstrong, S.J., and Franklin, F.C.H. (2011). Pathways to meiotic recombination in *Arabidopsis thaliana*. New Phytol. **190:** 523–544.

Page, S.L., and Hawley, R.S. (2001). c(3)G encodes a Drosophila synaptonemal complex protein. Genes Dev. **15:** 3130–3143.

Phillips, D., Nibau, C., Wnetrzak, J., and Jenkins, G. (2012). High resolution analysis of meiotic chromosome structure and behaviour in barley (*Hordeum vulgare* L.). PLoS ONE **7:** e39539.

Phillips, D., Wnetrzak, J., Nibau, C., Barakate, A., Ramsay, L., Wright, F., Higgins, J.D., Perry, R.M., and Jenkins, G. (2013). Quantitative high resolution mapping of HvMLH3 foci in barley pachytene nuclei reveals a strong distal bias and weak interference. J. Exp. Bot. **64:** 2139–2154.

Ronquist, F., and Huelsenbeck, J.P. (2003). MrBayes 3: Bayesian phylogenetic inference under mixed models. Bioinformatics **19:** 1572–1574.

Sanchez Moran, E., Armstrong, S.J., Santos, J.L., Franklin, F.C.H., and Jones, G.H. (2001). Chiasma formation in *Arabidopsis thaliana*

accession Wassileskija and in two meiotic mutants. Chromosome Res. **9:** 121–128.

Sanchez-Moran, E., Santos, J.L., Jones, G.H., and Franklin, F.C.H. (2007). ASY1 mediates AtDMC1-dependent interhomolog recombination during meiosis in *Arabidopsis*. Genes Dev. **21:** 2220–2233.

Sandhu, D., and Gill, K.S. (2002). Gene-containing regions of wheat and the other grass genomes. Plant Physiol. **128:** 803–811.

Scherthan, H. (2001). A bouquet makes ends meet. Nat. Rev. Mol. Cell Biol. **2:** 621–627.

Schwacha, A., and Kleckner, N. (1995). Identification of double Holliday junctions as intermediates in meiotic recombination. Cell **83:** 783–791.

Snowden, T., Acharya, S., Butz, C., Berardini, M., and Fishel, R. (2004). hMSH4-hMSH5 recognizes Holliday Junctions and forms a meiosis-specific sliding clamp that embraces homologous chromosomes. Mol. Cell **15:** 437–451.

Suzuki, M. (1989). SPXX, a frequent sequence motif in gene regulatory proteins. J. Mol. Biol. **207:** 61–84.

Sym, M., Engebrecht, J.A., and Roeder, G.S. (1993). ZIP1 is a synaptonemal complex protein required for meiotic chromosome synapsis. Cell **72:** 365–378.

Taketa, S., Ando, H., Takeda, K., and von Bothmer, R. (1999). Detection of *Hordeum marinum* genome in three polyploid *Hordeum* species and cytotypes by genomic in situ hybridization. Hereditas **130:** 185–188.

Tsubouchi, T., and Roeder, G.S. (2005). A synaptonemal complex protein promotes homology-independent centromere coupling. Science **308:** 870–873.

Van Bel, M., Proost, S., Wischnitzki, E., Movahedi, S., Scheerlinck, C., Van de Peer, Y., and Vandepoele, K. (2012). Dissecting plant genomes with the PLAZA comparative genomics platform. Plant Physiol. **158:** 590–600.

Wang, K., Wang, M., Tang, D., Shen, Y., Miao, C., Hu, Q., Lu, T., and Cheng, Z. (2012). The role of rice HEI10 in the formation of meiotic crossovers. PLoS Genet. **8:** e1002809.

Wang, M., Wang, K., Tang, D., Wei, C., Li, M., Shen, Y., Chi, Z., Gu, M., and Cheng, Z. (2010). The central element protein ZEP1 of the synaptonemal complex regulates the number of crossovers during meiosis in rice. Plant Cell **22:** 417–430.

Wijnker, E., et al. (2013). The genomic landscape of meiotic crossovers and gene conversions in *Arabidopsis thaliana*. Elife **2:** e01426.

Zhang, J., Pawlowski, W.P., and Han, F. (2013). Centromere pairing in early meiotic prophase requires active centromeres and precedes installation of the synaptonemal complex in maize. Plant Cell **25:** 3900–3909.

Zickler, D., and Kleckner, N. (1998). The leptotene-zygotene transition of meiosis. Annu. Rev. Genet. **32:** 619–697.

Zickler, D., and Kleckner, N. (1999). Meiotic chromosomes: Integrating structure and function. Annu. Rev. Genet. **33:** 603–754.